Journal of Catalysis 299 (2013) 10–19

Contents lists available at SciVerse ScienceDirect

Journal of Catalysis

journal homepage: www.elsevier.com/locate/jcat

Selective oxidation of alcohols to aldehydes/ketones over copper oxide-supported gold catalysts

Hui Wang [a], Weibin Fan [a,*], Yue He [a], Jianguo Wang [a], Junko N. Kondo [b], Takashi Tatsumi [b]

[a] State Key Laboratory of Coal Conversion, Institute of Coal Chemistry, Chinese Academy of Sciences, 27 South Taoyuan Road, Taiyuan 030001, China
[b] Catalytic Chemistry Division, Chemical Resources Laboratory, Tokyo Institute of Technology, Nagatsuta 4259, Midori-ku, Yokohama 226-8503, Japan

ARTICLE INFO

Article history:
Received 17 September 2012
Revised 2 November 2012
Accepted 7 November 2012
Available online 7 January 2013

Keywords:
Alcohol
Gold
Heterogeneous catalysis
Selective oxidation
Supported catalysts

ABSTRACT

Selective oxidation of alcohols to aldehydes/ketones with O_2 over a series of supported gold catalysts was studied. The catalytic performance depends strongly on the support. It is also strongly influenced by the preparation method and the pH value and stirring rate during the co-precipitation process as a result of their effect on the structure of the support and the particle size and electronic state of gold. The Au/CuO co-precipitated at pH 10 and stirring rate 100 rpm showed high activity, selectivity, and stability. The reaction might occur via oxidative dehydroxylation of alcohols to aldehydes/ketones by direct β-C—H elimination, as indicated by the IR result. The oxidation of different cycloalcohols showed that the activity increased with an increase in their methyl groups. Both conversion and ketone selectivity higher than 99% were achieved for cyclooctanol and cyclododecanol.

1. Introduction

Selective oxidation of alcohols to aldehydes or ketones has attracted a lot of attention because these products are important intermediates for the synthesis of fine chemicals, and it opens up the possibility of using renewable biomass-derived feedstocks [1–3]. Usually, toxic and/or homogeneous oxidants, for example, CrO_3, $KMnO_4$, MnO_2, SeO_2, and Br_2, are used stoichiometrically [1]. From the point of view of sustainable and green chemistry, these oxidants should be replaced with clean oxidants such as aqueous H_2O_2 and particularly molecular oxygen [2]. However, this requires preparation of highly active, selective, and recyclable O_2-activating heterogeneous catalysts [3].

In this context, noble metals such as Pt and Pd have been used to catalyze the oxidation of alcohols [4,5]. Although considerable progress has been made in the past two decades, the low catalytic stability or the quick catalyst deactivation arising from particle aggregation or leaching of noble metals during the reaction and/or regeneration process has still been a fatal problem limiting their wide industrial utilization [5,6]. This particularly holds true for the liquid-phase oxidation of alcohols with molecular oxygen over supported catalysts. Nevertheless, supported gold catalysts have recently been shown to be highly active and selective and more resistant to deactivation than Pt and Pd catalysts for the oxidation of alcohols and alkenes, although gold is traditionally regarded as an inert metal [10–13].

Galvagno et al. [7] reported that the catalytic properties of supported gold catalysts are strongly dependent on the types and structures of supports. By comparatively studying Fe_2O_3-, ZnO-, CaO-, and Al_2O_3-supported gold catalysts, they found that the basicity and lattice oxygen of supports have significant effects on the catalytic performance. They also demonstrated that addition of base to the reaction mixture is essential for achieving high activity [14] as a result of favoring abstraction of hydrogen from alcohols [9]. However, this is not true for the Au/CeO_2 catalyst, which showed high activity and selectivity in the oxidation of alcohols to aldehydes or ketones in the presence of O_2 without requirement of additional base [8,9]. The high catalytic activity of the Au/CeO_2 catalyst was ascribed to the stabilization of the positive oxidation states of gold through its interaction with the nanometric ceria surface, which creates Ce^{3+} and oxygen-deficient sites in the ceria, and consequently stabilizes the reactive peroxy intermediate formed from O_2 [15,16]. A further increase in the activity could be achieved by alloying Au and other noble metals such as Pd and Ag [17–19]. Hutchings et al. reported that Au—Pd alloy nanoparticles supported on TiO_2 showed much higher activity and selectivity than Au/TiO_2 and Pd/TiO_2 catalysts for the oxidation of a series of alcohols [3,4].

Although the preparation methods, the nature of supports, and the size of gold particles have been proved to affect the catalytic performance considerably [4,14,15], these factors have not been fully understood. This is because the catalytic reaction mechanism

---

* Corresponding author. Fax: +86 351 4050350.
E-mail address: fanwb@sxicc.ac.cn (W. Fan).

0021-9517/$ - see front matter © 2012 Elsevier Inc. All rights reserved.
http://dx.doi.org/10.1016/j.jcat.2012.11.018

remains unclear, although considerable progress has been made in the last decade. It is widely accepted that a synergetic effect might exist between the gold nanoparticles and the support. It was also suggested that hydroperoxy/peroxy intermediate species were possibly formed during the reaction [4,16,10]. This is supported by the finding that the addition of a peroxy initiator was necessary to start the epoxidation of cyclooctene with molecular oxygen [4]. In the case of oxidation of alcohols with O_2 over Au/TiO_2, the adsorption and activation of molecular oxygen could be enhanced by the hydroxyl groups formed through the dissociation of H_2 and H_2O molecules on the oxygen vacancies, possibly as a result of facilitating O_2 adsorption on TiO_2, and hence activating O_2 molecules [20]. This is supported by a substantial increase in activity in the presence of water. Nevertheless, to date, no unambiguous evidence has been obtained. Detailed mechanistic studies aiming at understanding why gold catalysts exhibit unique catalytic properties are required, since this would significantly promote the research progress of gold catalysis. Unfortunately, the papers concerning such mechanistic studies in recent years are few, probably because of extreme complexity.

In this work, a systematic study on the oxidation of alcohols with molecular oxygen over the supported gold catalysts was conducted. It shows that Au/CuO prepared by the co-precipitation method is a highly active, selective, and stable heterogeneous catalyst for the oxidation of alcohols to aldehydes or ketones, and that the preparation method, the pH value of the precipitation mixture, and the stirring rate in the co-precipitation process significantly influence the catalytic performance.

2. Experimental

2.1. Catalyst preparation

The supported gold catalysts were prepared by the co-precipitation, HCHO-reduction, boiling, physical mixture, and impregnation methods. The metal nitrates of $Cu(NO_3)_2{\cdot}3H_2O$, $Mn(NO_3)_2{\cdot}6H_2O$, $Ni(NO_3)_2{\cdot}6H_2O$, $Co(NO_3)_2{\cdot}6H_2O$, $Fe(NO_3)_3{\cdot}9H_2O$, $Cr(NO_3)_3{\cdot}9H_2O$, and $Al(NO_3)_3{\cdot}9H_2O$ were used to prepare the metal oxide supports of CuO, MnO_2, NiO, CoO_x, Fe_2O_3, Cr_2O_3, and Al_2O_3, respectively, while titanium tetra-butoxide monomer (TBOT) and tetraorthosilicate (TEOS) were used to prepare TiO_2 and SiO_2, respectively.

The preparation procedures for the co-precipitation method are as follows: a certain amount of metal nitrates or TEOS was first dissolved in distilled water, followed by the addition of aqueous $HAuCl_4$ solution. The resultant solution was then slowly adjusted to the designated pH value with 2.5 M aqueous NaOH solution under stirring conditions. The precipitated solid was centrifuged and washed several times with deionized water until no chlorine ions were detected by $AgNO_3$ solution. The resulting material was then dried at 100 °C to obtain the Au/CuO_{co}, Au/MnO_{2co}, Au/NiO_{co}, Au/CoO_{xco}, Au/Fe_2O_{3co}, Au/Cr_2O_{3co}, Au/Al_2O_{3co}, and Au/SiO_{2co} catalysts. The Au—Ag/CuO_{co} catalyst and the co-oxide-supported gold catalysts were prepared by the co-precipitation method with $AgNO_3$, TBOT, and TEOS as the Ag, TiO_2, and SiO_2 sources, respectively. The MCM-41 was formed through hydrolysis of TEOS in the presence of cetyltrimethylammonium bromide (CTAB).

The preparation procedures for the boiling method are simple. Aqueous $Cu(NO_3)_2{\cdot}3H_2O$ and $HAuCl_4$ solution were refluxed for 1 h under boiling conditions. Then, the solid was separated, washed, and dried at 100 °C to obtain the catalyst of Au/CuO_{boil}. If the solution was first boiled for 0.5 h, and then aqueous HCHO solution (37%) was added and further boiled for another 0.5 h, followed by centrifuging, washing, and drying at 100 °C, we called this the HCHO-reduction method in order to distinguish it from the boiling method. The catalyst prepared by this method was designated as Au/CuO_{HCHO}.

For the physical mixture method, the pH value of aqueous $HAuCl_4$ solution was adjusted to 10. Then, CuO precipitated at the same pH value was added and the mixture was stirred for 20 min. Finally, the solid was separated by centrifuging, washed with distilled water, and dried at 100 °C to obtain the Au/CuO_{phy} catalyst.

For comparison, an Au/CuO catalyst was also prepared by the incipient wetness impregnation method at ambient temperature with aqueous $HAuCl_4$ solution as Au precursor. The catalysts were then dried at 100 °C, and the obtained sample was designated as Au/CuO_{im}.

2.2. Catalyst characterization

XRD was performed on an advanced X-ray diffractometer (Bruker AXS D8, Germany). The diffraction patterns of the samples were recorded at room temperature with Cu Kα radiation in the range of 2θ between 10° and 80°. The HRTEM images of the samples were obtained on a JEM 2010 microscope operated at 200 kV and equipped with an energy-dispersive X-ray (EDX) instrument. The X-ray photoelectron spectra (XPS) were measured on a Shimadzu ESCA 3200 X-ray photoelectron spectrometer equipped with an Mg Kα target. About 70 mg of the sample was compressed into a self-supported wafer for analysis. The survey spectra were measured in a binding energy (BE) range of 0–1100 eV. The BE was calibrated with the C1*s* signal located at 284.6 eV. The data analysis involved spectral normalization, Shirley background correction, and curve fitting by Gaussian–Lorentzian functions. The Au4*f* regions were fitted by doublets with fixed spectroscopic parameters, for example, of the $4f_{5/2}$ to $4f_{7/2}$ branch ratio of 3–4, but the full width at half maximum (FWHM), positions, and intensities of the signals are independent and variable, and optimized by the above-mentioned fitting program.

IR measurements were carried out on a Jasco FTIR 7300 spectrometer with an MCT detector at a resolution of 2 cm^{-1} by accumulating 64 scans. Prior to the measurement, the sample was treated at 100 °C under high-vacuum conditions (<1 Pa) to remove adsorbed water and organics. After it was cooled in situ to room temperature, the spectrum was collected. Then, the sample was allowed to adsorb benzyl alcohol vapor for 10 min. This was followed by evacuation to 1 Pa and collecting the spectrum again. Subsequently, the sample was treated with O_2 (200 Pa) to oxidize adsorbed benzyl alcohol, and the spectrum was recorded at a different reaction time.

2.3. Catalytic tests

The liquid-phase oxidation of alcohols with O_2 in the presence or absence of solvent was conducted at atmospheric pressure in a round-bottom flask (50 mL) equipped with a condenser under stirring conditions. The temperature was controlled with a water bath and kept at 70 or 80 °C. The reaction time was 5–20 h. The detailed reaction conditions for different batches are shown in the footnotes of tables and the captions of figures. The obtained products were analyzed on two GC-14B gas chromatographs equipped with flame ionization detectors and a 50-m OV-1 and a 30-m PEG capillary column, respectively.

3. Results and discussion

3.1. Effect of supports on the oxidation of benzyl alcohol with O_2 over the supported gold catalysts

Table 1 shows the catalytic results obtained over a series of supported gold catalysts prepared by the co-precipitation method in

Table 1
Catalytic results for the oxidation of benzyl alcohol with O_2 over various supported gold catalysts prepared by the co-precipitation method.

Catalysts	Au (wt.%)	Conversion (%)	Selectivity (%)		TOF (h^{-1})[a]
			Benzaldehyde	Others	
CuO_{co}	–	1.6	>99	n.d.	–
Au/CuO_{co}	4.0	58.5	98.2	1.8	56
Au/MnO_{2co}	5.1	12.2	87.7	12.3	8
Au/NiO_{co}	4.4	40.7	68.7	31.3	25
Au/CoO_{xco}	4.3	28.7	71.6	28.4	19
Au/Fe_2O_{3co}	6.8	35.0	72.1	27.9	15
Au/Cr_2O_{3co}	2.8	3.3	94.8	5.2	4
Au/Al_2O_{3co}	3.9	30.0	53.1	46.9	16
Au/SiO_{2co}	3.3	30.1	62.1	37.9	23

Note: Reaction conditions: 0.1 g catalyst, 10 mmol benzyl alcohol, 80 °C, 5 h, 5 mL/min O_2.

[a] TOF was calculated on the basis of total loading of gold.

Table 2
Effects of different co-supports or co-active component of Ag on the catalytic performance of Au/CuO_{co}.

Catalysts	Au (wt.%)	Conversion (%)	Selectivity (%)		TOF[a] (h^{-1})
			Benzaldehyde	Others	
Au/3%CuO–1%TiO_2	5.5	2.5	>99	n.d.	0.1
Au/1%CuO–3%MCM-41	2.7	73.0	94.3	5.7	7.4
Au/1%CuO–1%MCM-41	2.9	49.1	97.4	2.6	4.9
Au/3%CuO–1%MCM-41	2.5	8.0	>99	n.d.	0.9
Au/1%CuO–3%MCM-41[b]	2.7	33.6	>99	n.d.	3.6
Au/1%CuO–3%MCM-41[c]	2.7	9.8	>99	n.d.	1.1
Au/1%CuO–1%MCM-41[b]	2.9	11.6	>99	n.d.	1.2
Au/1%CuO–1%MCM-41[c]	2.9	3.2	>99	n.d.	0.3
Au(6%)–Ag(3%)/CuO	4.7	0.9	>99	n.d.	0.1
Au/MCM-41	3.4	71.1	92.2	7.8	5.6

Note: Reaction conditions: 0.1 g catalyst, 10 mL toluene, 3 mmol substrate, 5 mL/min O_2, 80 °C, 20 h.

[a] TOF was calculated on the basis of total loading of gold.

[b] Extracted with anhydrous ethanol.

[c] Extracted with 0.2 M HCl ethanol solution.

the oxidation of benzyl alcohol to benzaldehyde with O_2 in the absence of solvent. The main by-products were benzoic acid and benzoic acid benzyl ester for all the catalysts. The Au/MnO_{2co} and Au/Cr_2O_{3co} catalysts gave turnover frequencies (TOF) of 8 and 4 h^{-1} and benzaldehyde selectivities of 87.7% and 94.8%, respectively. When the Au/NiO_{co}, Au/Fe_2O_{3co}, Au/CoO_{xco}, Au/Al_2O_{3co}, and Au/SiO_{2co} catalysts were used, the TOF increased to 15–25 h^{-1}, although the selectivities to benzaldehyde decreased to 53.1–72.1%. As for Au/CuO_{co} catalyst, a conversion of 58.5% was obtained at the reaction time of 5 h, which corresponds to a TOF of 56 h^{-1}. Meanwhile, the selectivity to benzaldehyde reached 98.2%. These results demonstrate that CuO is an effective support for the gold catalyst in the selective oxidation of benzyl alcohol with molecular oxygen. However, CuO itself is nearly inactive in this reaction. This reveals that Au plays a major role in catalyzing this reaction, or that Au and CuO collaboratively catalyze this reaction.

In order to further increase the activity of the Au/CuO_{co}, the effects of the co-support or the co-active metal on the catalytic performance of Au/CuO were investigated. Table 2 lists the catalytic results obtained over various gold catalysts with co-supports or co-active components. It is unexpected that the introduction of the co-supports of TiO_2 and MCM-41 or the co-active metal of Ag led to a decrease in activity to the TOFs less than 10 h^{-1}. Very low conversion was obtained over the $Au/(CuO + TiO_2)_{co}$ even if the reaction time was increased to 20 h. This is probably due to the reduction of CuO to Cu, as indicated by the bronze color of the precipitation. For the Au—Ag/CuO catalyst, it was also nearly inactive for the oxidation of benzyl alcohol with O_2, probably as a result of the formation of AgCl when Au and Ag were simultaneously co-precipitated on the CuO support.

When MCM-41 served as a support, a conversion of 71.1% was obtained, although the benzaldehyde selectivity decreased to 92.2%. This suggests that the addition of MCM-41 to the Au/CuO_{co} catalyst would possibly increase the catalytic activity. Thus, the ratio of CuO to MCM-41 was adjusted further to improve the catalytic performance. It was found that the benzyl alcohol conversion increased from 8.0% to 73.0% when the CuO/MCM-41M ratio decreased from 3/1 to 1/3 (Table 2). Irrespective of this, a further increase in MCM-41 had no positive effect. The as-synthesized MCM-41-supported Au catalyst gave a conversion of benzyl alcohol and a selectivity of benzaldehyde similar to those obtained over the Au/CuO_{co}–MCM-41 catalyst with a CuO/MCM-41M ratio of 1/3. Attempt to remove CTAB surfactant by Soxhlet extraction with anhydrous ethanol led to a decrease in the benzyl alcohol conversion to 33.6%. A much more significant decrease in the benzyl alcohol conversion was observed when the surfactant was removed by extraction with 0.2 M HCl ethanol solution. This results from severe leaching of gold nanoparticles during the extraction process.

It was reported that the presence of base favored the selective oxidation of alcohols over the supported gold catalysts [9,14]. Thus, a certain amount of Na_2CO_3, K_2CO_3, or K_3PO_4 was added to the reaction mixture of oxidation of benzyl alcohol with molecular oxygen over the Au/CuO_{co}, and the obtained catalytic results are shown in Table 3. Unexpectedly, addition of alkali metal salts to the reaction mixture had a negligible or a negative effect on the catalytic performance. When Na_2CO_3 was added, although the activity increased slightly, the selectivity of benzaldehyde was reduced by 2.6%, which might be due to the promotion of the esterification reaction. An increase in the basicity of added alkali metal salts conversely decreased the catalytic activity. Thus, the addition of a base to the reaction mixture is not beneficial or even detrimental to the oxidation of benzyl alcohol over the Au/CuO$_{co}$. Nevertheless, the leaching of CuO was completely inhibited by the addition of base, as confirmed by the fact that the reaction liquid changed from green under the solvent-free condition to colorless when Na_2CO_3 was added.

Table 3
Effect of the base added to the reaction mixture on the catalytic performance of Au/CuO$_{co}$ for the oxidation of benzyl alcohol with O_2.

Bases	Conversion (%)	Selectivity (%)		TOF (h^{-1})[a]
		Benzaldehyde	Others	
No	45.3	98.7	1.3	87.6
Na_2CO_3	47.8	96.1	3.9	90.0
Na_3PO_4	38.8	94.4	5.6	71.8
K_3PO_4	26.3	95.6	4.4	49.3

Note: Reaction conditions: 0.1 g catalyst, 80 °C, 5 h, 20 mmol benzyl alcohol, 5 mL/min O_2, 0.6 g alkali metal salt.

[a] TOF was calculated on the basis of total loading of gold.

Table 4
Catalytic results for the oxidation of benzyl alcohol with O_2 over Au/CuO catalysts prepared by different methods.

Preparation method	Au (wt.%)	Conversion (%)	Selectivity (%)		TOF (h^{-1})[a]
			Benzaldehyde	Others	
Co-precipitation	4.0	85.7	>99	n.d.	6.2
Boiling 0.5 h + HCHO reduction + boiling 0.5 h	0.27	2.6	>99	n.d.	2.8
Boiling 1.0 h	1.1	17.1	>99	n.d.	4.6
Physically mixing	3.2	56.1	>99	n.d.	5.1
Impregnation	6.0	1.5	>99	n.d.	0.1

Note: Reaction conditions: 0.1 g catalyst, 80 °C, 20 h, 3 mmol benzyl alcohol, 10 mL toluene, 5 mL/min O_2.

[a] TOF was calculated on the basis of total loading of gold.

3.2. Effect of preparation parameters on the oxidation of benzyl alcohol with O_2 over Au/CuO

3.2.1. Effect of preparation methods

Table 4 summarizes the catalytic results obtained over the Au/CuO samples prepared by the co-precipitation, boiling, HCHO-reduction, physical mixture, and impregnation methods in the oxidation of benzyl alcohol with molecular oxygen. Clearly, the preparation method had a strong influence on the catalytic performance of the Au/CuO. Although the selectivity of benzaldehyde was higher than 99% for all the prepared samples, the activities are markedly different. The Au/CuO$_{co}$ sample showed a high conversion of 85.7%, whereas the Au/CuO$_{HCHO}$ and Au/CuO$_{im}$ gave a conversion lower than 3%. In the case of Au/CuO$_{boil}$ and Au/CuO$_{phy}$, moderate conversions were obtained as a result of both having low Au content. This is supported by the TOF obtained over these two catalysts, which is similar to that of Au/CuO$_{co}$. The low activity of the Au/CuO$_{im}$ is probably due to the presence of large amounts of chlorine ions, which was considered to poison gold catalysts [11].

Fig. 1 shows the XPS spectra and their deconvoluted configurations of the Au/CuO catalysts prepared by the different methods in the BE range for Au4*f* signals. The binding energies of bulk metallic Au, Au_2O_3, and $Au(OH)_3$ are 83.9, 86.3, and 87.7 eV for $4f_{7/2}$ and 87.7, 89.6, and 91.4 eV for $4f_{5/2}$, respectively [22–25]. The very small (nonmetallic) Au cluster or Au^+ peaks locate at 84.9 and 88.6 eV [26–28]. Thus, it can be deduced that the Au/CuO$_{im}$ contains mainly bulk metallic Au and Au_2O_3, whereas the Au/CuO$_{co}$ contains mainly Au_2O_3, $Au(OH)_3$, and Au^+ and/or nonmetallic Au clusters, but few metallic Au, since no signal was observed around 83.9 eV. For the Au/CuO$_{boil}$, both bulk Au and nonmetallic Au clusters are present. In the case of Au/CuO$_{HCHO}$ and Au/CuO$_{phy}$, no obvious signals characteristic of Au species were observed because of their very low Au content (<0.3%).

Table 4 shows that the Au/CuO$_{boil}$ showed a TOF of 4.6 h^{-1}, lower than that (6.2 h^{-1}) of the Au/CuO$_{co}$. This indicates that besides

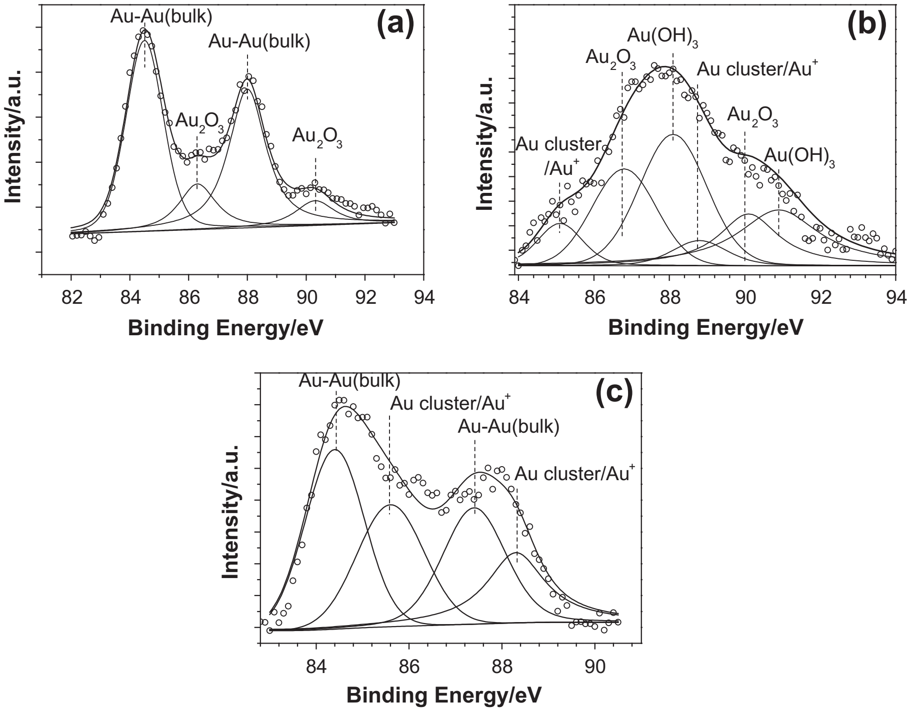

Fig. 1. XPS spectra and the deconvoluted configurations of Au4*f* signals of the Au/CuO prepared by the (a) impregnation, (b) co-precipitation, and (c) boiling methods.

Table 5
Effects of the pH value of the co-precipitated gel on the catalytic performance of prepared Au/CuO$_{co}$ for the oxidation of benzyl alcohol with O_2.

pH value	Au (wt.%)	Conversion (%)	Selectivity (%)		TOF (h^{-1})[a]
			Benzaldehyde	Others	
8	4.7	39.7	27.7	72.3	0.7
9	5.0	16.4	>99	n.d.	1.0
10	4.0	85.7	>99	n.d.	6.3
11	4.0	76.7	>99	n.d.	5.6

Note: Reaction conditions: 0.1 g catalyst, 80 °C, 20 h, 3 mmol benzyl alcohol, 10 mL toluene, 5 mL/min O_2.

[a] TOF was calculated on the basis of total loading of gold.

the Au content and the chlorine ions, the gold electronic state may strongly influence the reactivity of Au/CuO, too. The higher activity of the Au/CuO$_{co}$ than of the Au/Cu$_{boil}$ might be due to the presence of abundant cationic (nonmetallic) Au species originated from the metal–support interaction [12]. The gold atoms interacted with the oxide support to form nonmetallic Au clusters or bond to surface hydroxyl or lattice/surface oxygen to form Au$^+$ and Au^{3+} species [15,16]. The interaction between the gold and the oxide support depends strongly on how the gold atoms arranged in the support [26], which is closely related to the preparation methods.

3.2.2. Effect of the pH value of the co-precipitated mixture

For the gold catalyst prepared by the co-precipitation method, the pH value of the co-precipitated mixture has a significant influence on the electronic state and particle size of gold and the structure of support [13,14]. Table 5 displays the catalytic results obtained over the Au/CuO$_{co}$ catalysts co-precipitated at pH values of 8, 9, 10, and 11 in the oxidation of benzyl alcohol with molecular oxygen. TOF increased with increasing pH value of the co-precipitated mixture up to 10. The selectivity of benzaldehyde was 27.7% when the pH value of the co-precipitated mixture was 8, while it reached more than 99% over the sample co-precipitated at pH 10. Nevertheless, a further increase in the pH value of the co-precipitated mixture decreased the benzyl alcohol conversion despite the fact that the benzaldehyde selectivity was still higher than 99%.

Fig. 2 shows the HRTEM images of the Au/CuO$_{co}$ samples co-precipitated at pH 8, 9, 10, and 11. The Au particles were homogeneously distributed on the CuO for all the four samples. Their sizes centered at 1–3, 3–6, 3–6, and 6–9 nm for the samples co-precipitated at pH 8, 9, 10, and 11, respectively. The size of the gold particles is one of the key factors that determine the activity of supported gold catalysts. The Au–oxygen interaction is highly dependent on the gold particle size at the nanoscale, which results in an interesting size selectivity in heterogeneously catalyzed reactions [15]. Generally, small gold particles enhance oxidation ability by facilitating oxygen activation [16]. Thus, the Au/CuO$_{co}$ catalyst precipitated at pH 8 showed low selectivity for benzaldehyde because its gold particles were in the range 1–3 nm, which could further oxidize the aldehyde to benzyl acid and subsequently form esters. As for the Au/CuO$_{co}$ catalysts precipitated at pH 9, 10, and 11, they had moderately large particles and consequently were highly selective for the oxidation of benzyl alcohol to benzaldehyde due to the inhibition of deep oxidation of benzaldehyde. This shows that gold particles larger than 3 nm seem not to be active for the further oxidation of benzaldehyde to benzoic acid.

The XRD patterns of the Au/CuO$_{co}$ co-precipitated at pH 8, 9, 10, and 11 are shown in Fig. 3. The Au/CuO$_{co}$ co-precipitated at pH 8 showed sharp diffraction lines at 2θ of 13.3°, 25.7°, 33.6°, and 58.1°. All these lines could be attributed to crystalline $Cu(OH)_2{\cdot}H_2O$

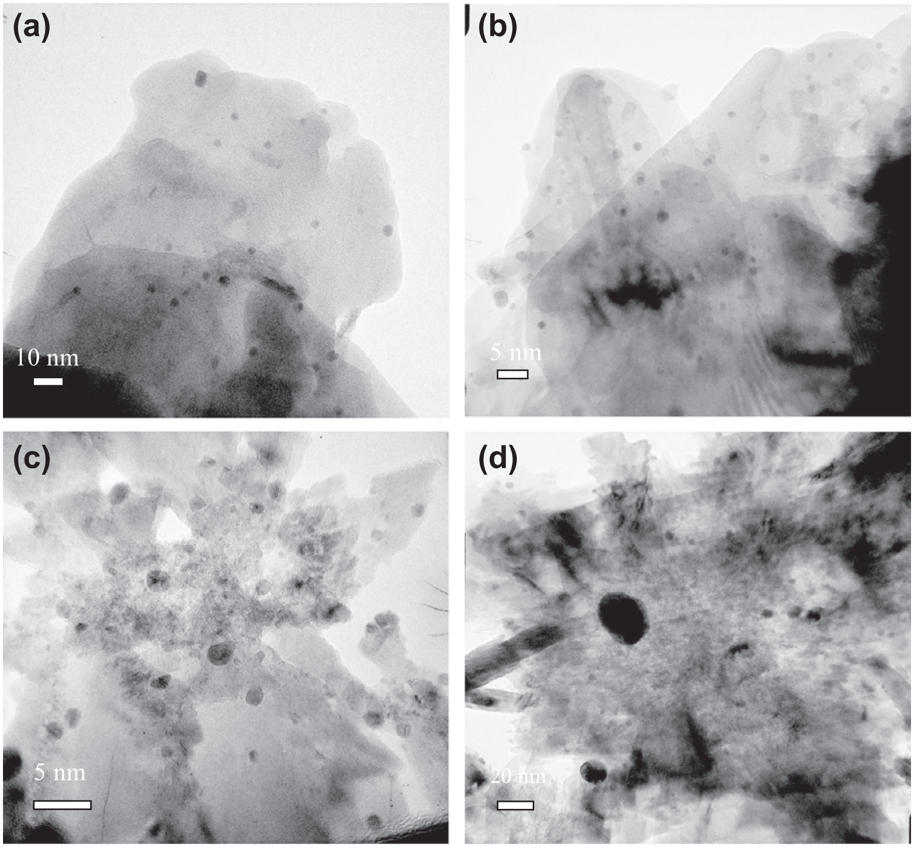

Fig. 2. HRTEM images of Au/CuO$_{co}$ catalysts co-precipitated at pH (a) 8, (b) 9, (c) 10, and (d) 11.

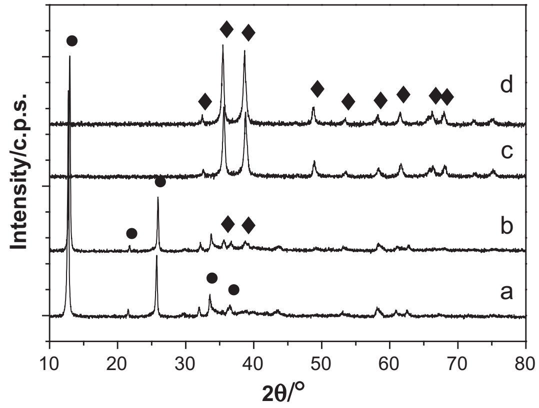

Fig. 3. XRD patterns of Au/CuO_{co} catalysts co-precipitated at pH (a) 8, (b) 9, (c) 10, and (d) 11. Crystalline phases detected: ♦ CuO; ● $Cu(OH)_2 \cdot H_2O$.

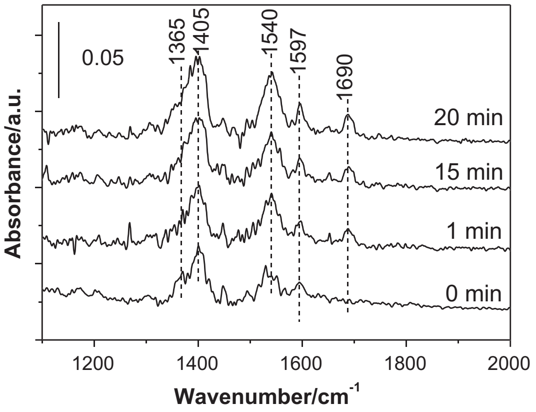

Fig. 5. IR spectra collected following the oxidation of benzyl alcohol with O_2 over the Au/CuO_{co} catalyst co-precipitated at pH 10: adsorption of benzyl alcohol (0 min) and further reaction with O_2 for 1 min, 15 min, and 20 min.

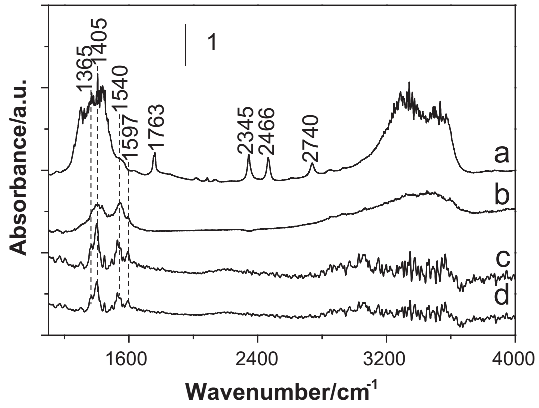

Fig. 4. IR spectra of the adsorption of benzyl alcohol over Au/CuO_{co} catalysts co-precipitated at the pH of (a) 8, (b) 9, (c) 10, and (d) 11.

(PDF number 42-0746). However, when the pH value of the co-precipitated mixture was increased to 9, these diffraction lines decreased in intensity, while new lines (at 2θ of 35.5°, 38.7°, and 48.8°) characteristic of CuO (PDF number 45-0937) appeared. This indicated that part of $Cu(OH)_2 \cdot H_2O$ transformed into CuO. A further increase in the pH of the co-precipitation mixture to 10 led to the complete transformation of $Cu(OH)_2 \cdot H_2O$ into CuO. This is coincident with the color change of the precipitation mixture from light green to black. XRD measurements demonstrated that the support co-precipitated at pH 11 was also pure CuO. On the other hand, no evident diffraction lines characteristic of gold species were detected for the four samples, showing that gold species were highly dispersed on the supports for all of these samples. Nevertheless, the HRTEM analysis indicated the presence of a larger number of 6–9 nm gold particles on the sample co-precipitated at pH 11. This part of the gold particles exhibited lower activity. The above results show that the pH value of the co-precipitated mixture influences not only the gold particle size but also the support structure and consequently the catalytic properties of the Au/CuO_{co} in the oxidation of alcohols with molecular oxygen.

Fig. 4 depicts the IR spectra of benzyl alcohol adsorbed on these four catalysts. The Au/CuO_{co} co-precipitated at pH 8 showed four bands at 1763, 2345, 2466, and 2740 cm^{-1}, which may be due to the formation of carboxylic acid and phenyl ester [17,18]. This shows that benzyl alcohol could be oxidized to acid and further to ester although no O_2 was introduced. This could be attributed to the strong oxidation ability of the small gold particles, which can catalyze the reaction between benzyl alcohol and the surrounding O—H on the catalyst. In addition, another two broad bands were observed in the regions 1200–1600 cm^{-1} and 3000–3600 cm^{-1}. These two bands are related to phenyl groups and O—H species [19,20]. When benzyl alcohol adsorbed on the surface of the Au/CuO_{co} was obtained at pH 9, these bands decreased greatly in intensity. This indicates that the adsorption of benzyl alcohol on the sample co-precipitated at pH 9 is significantly weaker than that on the sample co-precipitated at pH 8. Although the bands between 1200 and 1600 cm^{-1} were more resolved and the broad band attributed to the hydrogen-bonded OH species was lower in intensity, similar IR spectra were obtained for the catalysts co-precipitated at pH 10 and 11. However, after penetration of O_2 for 10 min, the band attributed to C=O-related species (—CHO) appeared at 1690 cm^{-1} [17] in the IR spectra of the Au/CuO_{co} co-precipitated at pH 10 (Fig. 5), while this band cannot be differentiated from the spectrum of the sample obtained at pH 9. It should be noted that no evidence was found for the occurrence of deep oxidation for the three samples. Thus, it is not difficult to understand that the sample co-precipitated at pH 8 showed a low benzaldehyde selectivity of 27.7%, while those co-precipitated at pH 9, 10, and 11 gave benzyl aldehyde selectivity higher than 99% and that co-precipitated at pH 9 showed a low conversion of 16.4%.

3.2.3. Effect of the stirring rate during the co-precipitation process

Like the pH value of the co-precipitated mixture, the stirring rate during the co-precipitation process also strongly affects the size of gold particles, although this point has not been received much attention. Fig. 6 shows the HRTEM imagines of the samples co-precipitated at different stirring rates. The samples co-precipitated at the stirring rates of 50 and 100 rpm had a narrow size distribution of gold nanoparticles, being approximately in Gauss distribution with average values of 4.3 and 4.5 nm, respectively. However, when the stirring rate was 50 rpm, CuO particle aggregation was observed to some extent. An increase in the stirring rate resulted in not only an increase in the gold particle size but also a broadening of the size distribution. The sample co-precipitated at a stirring rate of 300 rpm had a gold particle size mainly in the ranges of 3–6 and 7–19 nm. When the stirring rate was increased to 500 rpm, most of the gold particles increased to 7–13 and 14–17 nm, although the average size (≈12 nm) was not significantly increased.

Table 6 shows the catalytic results of the Au/CuO_{co} catalysts co-precipitated at stirring rates of 50, 100, 300, and 500 rpm. The function for benzyl alcohol conversion vs. stirring rate showed a volcanic shape despite the fact that the benzaldehyde selectivity

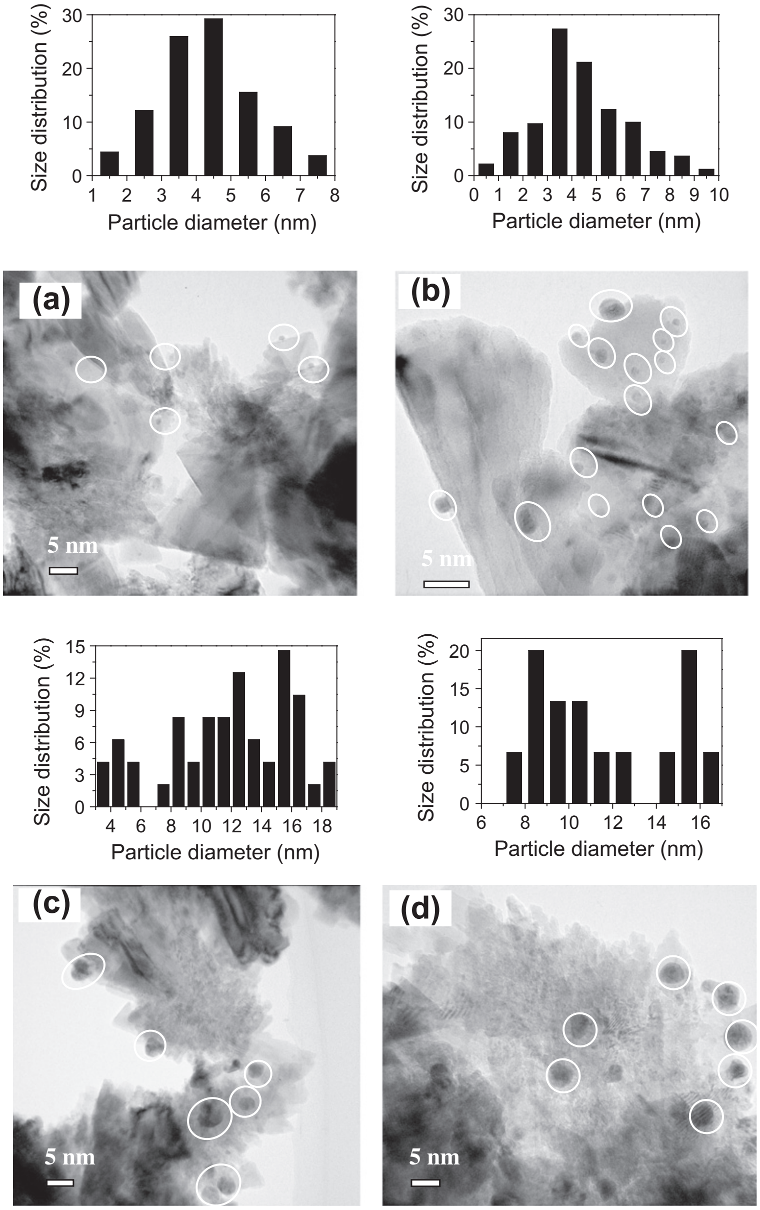

Fig. 6. HRTEM images and gold particle size distribution of the Au/CuO$_{co}$ catalysts co-precipitated at the stirring rate of (a) 50 rpm, (b) 100 rpm, (c) 300 rpm, and (d) 500 rpm.

was higher than 99% for all the samples, as the sizes of most of their gold particles were larger than 3 nm. The sample precipitated at 100 rpm gave the highest conversion, 85.7%. A decrease or an increase in the stirring rate led to a reduction in benzyl alcohol conversion.

The precipitation is a complex process, including the primary process of nucleation, growth, and dissolution of a metastable phase and the secondary process of nucleation and growth of a stable phase [21]. The kinetics of nucleation and growth of each phase determines which phase appears first and how long the transformation from the metastable form to the stable phase takes. The overall kinetics results from a complex interplay between the nucleation, the growth, and the dissolution of the involved solids. Cornel et al. studied the effect of the stirring rate on the transformation process using a population balance model [22]. It was found that the stirring rate integration controlled the growth of the metastable phase. Thus, an integration mechanism in which the growth of the stable phase would be limited at low supersaturation in a stirring vessel was assumed, where the nucleation time of the stable phase was strongly influenced by the stirring rate [22]. Such a mechanism might dominate the co-precipitation process of the Au/CuO$_{co}$ catalyst, since this process occurred in the stirring system with low supersaturation. The low stirring rate favors the nucleation of the metastable phase but limits the growth of the stable form, giving small gold particles. An increase in the

Table 6
Effects of the stirring rate during the co-precipitation process on the catalytic performance of Au/CuO$_{co}$ in the oxidation of benzyl alcohol with O$_2$.

Stirring rate (rpm)	Conversion (%)	Selectivity (%)	
		Benzaldehyde	Others
50	47.4	>99	n.d.
100	85.7	>99	n.d.
300	62.5	>99	n.d.
500	51.4	99.3	0.7

Note: Reaction conditions: 0.1 g catalyst, 10 mL toluene, 3 mmol benzyl alcohol, 5 mL/min O$_2$, 80 °C, 20 h.

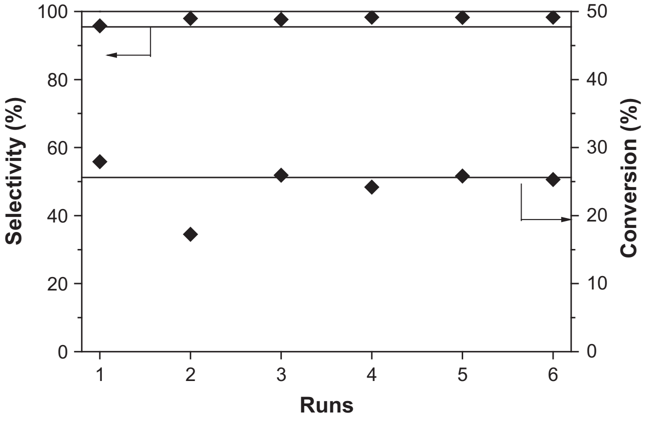

Fig. 7. Catalytic results for the oxidation of benzyl alcohol with O_2 over the Au/CuO$_{co}$ catalyst within six repeated runs with regeneration (reaction conditions: catalyst/Na_2CO_3/substrate = 0.1 g/0.3 g/20 mmol, 80 °C, 5 h, 5 mL/min O_2).

stirring rate not only led to a remarkable decrease in the nucleation time of the stable phase but also promoted its crystal growth. When the stirring rate was increased to a certain value, a population balance was established between the dissolution of the metastable phase and the nucleation and growth of the stable form. As a result, no obvious increase in the average size was observed for gold particles.

3.3. Catalytic recyclability of the Au/CuO$_{co}$ in the oxidation of benzyl alcohol with O_2

Fig. 7 shows the catalytic results for Au/CuO$_{co}$ in the oxidation of benzyl alcohol with O_2 under the same reaction conditions in the presence of Na_2CO_3 in six repeated runs with regeneration. Clearly, Au/CuO$_{co}$ showed similar benzyl alcohol conversion and benzaldehyde selectivity for all the runs, except for the second recycle. This shows that the prepared Au/CuO$_{co}$ catalyst is highly stable during the reaction process. This is also supported by the facts that the reaction liquid was kept colorless after filtration of the catalyst and that no leaching of gold particles was detected by ICP. The decrease in benzyl alcohol conversion from 27.9% to 17.2% in the second run is due to the regeneration method employed. If the Au/CuO$_{co}$ was regenerated by washing with only acetone for three times, as done in the case of run 2, its catalytic activity significantly decreased. However, when the spent catalyst was washed with water and subsequently with acetone for three times each, as done in the runs 3–6, its catalytic reactivity was recovered. This shows that accumulation of organic and inorganic species adsorbed on its surface caused its deactivation, suggesting that the decrease in activity with the alkalinity of the added base may be due to the increased adsorption of organic and inorganic species onto the surface of the catalyst (Table 3). The effective regeneration method for the spent Au/CuO$_{co}$ is to clean its surface by thoroughly washing it with both the inorganic solvent water and the organic solvent acetone.

It is interesting that although part of the CuO was transformed into Cu_2O after each run, as revealed by XRD measurements, it was mostly reoxidized to CuO again after regeneration and drying (Fig. 8). This demonstrates that the CuO support participated in the oxidation reaction. Also, it is worth noting that no diffraction peaks characteristic of gold species are detected in all the spent catalysts, indicating that the high dispersion of Au on the support was maintained during the regeneration and reaction processes.

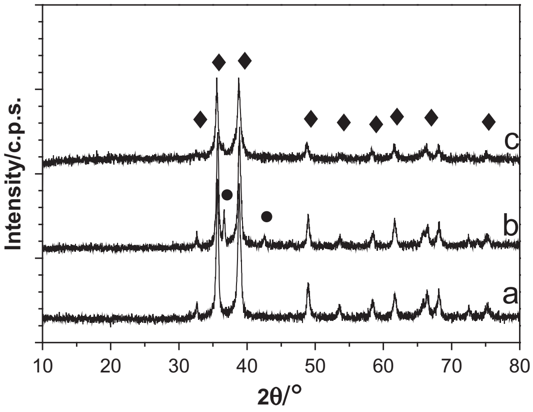

Fig. 8. XRD patterns of the fresh (a), spent (b), and regenerated (c) Au/CuO$_{co}$ catalyst: ♦ CuO; ● Cu_2O.

3.4. Catalytic mechanism of oxidation of benzyl alcohol by O_2 over Au/CuO$_{co}$

Fig. 5 shows the IR spectra collected at 1, 15, and 20 min for the oxidation of benzyl alcohol by molecular oxygen over the Au/CuO$_{co}$ co-precipitated at pH 10. When benzyl alcohol adsorbed onto the surface of the sample, four bands at 1597, 1540, 1405, and 1365 cm^{-1} were observed in the IR spectrum. The band at 1597 cm^{-1} was due to the C=C vibration of the phenyl ring [23], whereas those at 1540 and 1405 cm^{-1} were attributed to the asymmetric and the symmetric stretching vibrations of the adsorbed O—C—O groups in bridge mode [17]. After O_2 was introduced, the band at 1365 cm^{-1}, ascribed to the scissor vibration of CH_2, disappeared, while a new band at 1690 cm^{-1} was observed, and increased in intensity with increasing reaction time. This demonstrates that benzyl alcohol was oxidized to benzaldehyde. However, this does not hold true for the pure CuO support as catalyst, on which benzaldehyde was not formed after O_2 treatment, although benzyl alcohol could adsorb weakly onto its surface. This is confirmed by the absence of the 1690 cm^{-1} band in the IR spectrum of the O_2-purged sample (Fig. 1S). This might be because benzyl alcohol adsorbed onto the surface of CuO so weakly that it could not be activated, and/or the pure CuO support could not activate the O_2 molecule. As a result, very low conversion (1.6%) was obtained on CuO (Table 1).

XRD measurements show that part of the CuO in the fresh Au/CuO$_{co}$ catalyst was reduced to Cu_2O after reaction and mostly recovered after regeneration (Fig. 8), indicating that the CuO support participated in the reaction through supply of active oxygen. The interaction between Au and CuO enhances the oxygen mobility and facilitates the formation of oxygen vacancy through the redox of $Au^0 \leftrightarrow Au^{\delta+}$ and CuO ↔ Cu_2O. In combination with the FTIR and XPS spectral and catalytic results, this suggests that the gold species and the CuO support collaboratively promoted the activation of benzyl alcohol and O_2. Thus, a possible mechanism, shown in Fig. 9, is proposed for the oxidation of benzyl alcohol over the Au/CuO$_{co}$ by modifying the conventional dehydrogenation mechanism [24,25]. Au acts as the sole catalytic center where reaction takes place, and the oxygen transfer is completed through the redox cycle of $Au^0 \leftrightarrow Au^{\delta+}$ and CuO ↔ Cu_2O. Benzyl alcohol molecules adsorbed onto the Au nanoparticles, forming metal–alkoxide intermediates and adsorbed hydrogens via O—H bond cleavage. The adsorbed hydrogen bonded to the surface lattice oxygen to form surface O—H, which is coordinated to the carbon atom of the methyl group in the benzyl alcohol molecule and accompanied by the transformation of CuO to Cu_2O. Hence, the O—C—O group in

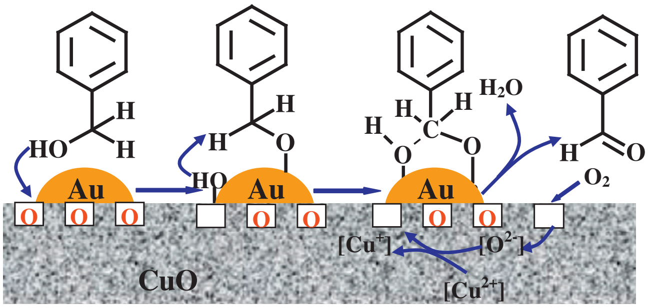

Fig. 9. Proposed reaction mechanism for the oxidation of benzyl alcohol by O_2 over the Au/CuO_{co} catalyst.

Table 7
Catalytic results for the oxidation of a variety of alcohols with O_2 over Au/CuO_{co}.

Entry	Substrate	Conversion (%)	Selectivity (%)	
			Aldehyde/ ketone	Others
1	Benzyl alcohol[a]	85.7	>99	n.d.
2	Cinnamyl alcohol[a]	83.8	99.4	0.6
3	Cyclohexanol[b]	66.0	>99.0	n.d.
4	Cyclooctanol[b]	99.0	>99.0	n.d.
5	Cyclododecanol[b]	>99.0	>99.0	n.d.
6	2-Methyl benzyl alcohol[a,c]	85.3	>99.0	n.d.
7	4-Methyl benzyl alcohol[a,c]	87.7	>99.0	n.d.
8	4-Methyl cyclohexanol[b]	71.4	>99.0	n.d.
9	3,5-Aimethyl cyclohexanol[b]	92.3	>99.0	n.d.

Notes: Reaction conditions: 0.1 g catalyst, 5 mL/min O_2, 10 mL toluene, [a]3 or [b]-2 mmol substrate, 80 or [c]70 °C, 20 h.

bridge mode was observed by IR. Finally, the C—H bond in the β position was activated, leading to the formation of benzaldehyde and water [26,27]. This is consistent with the finding of Mullins et al. that the β-H elimination mechanism dominates the dehydroxylation of alcohols to aldehydes or ketones over bulk gold catalyst [28]. The oxygen adsorbed onto the support surface disassociates into chemisorbed oxygen species and diffuses into the support lattice vicinity. This is followed by activation at the oxygen vacancies and conversion into lattice oxygen O^{2-}. The lattice oxygen further transferred to the surface of CuO through oxygen-deficient sites, restoring the interface between the support and Au active sites, and reacted with benzyl alcohol, as shown in Fig. 9.

3.5. Oxidation of a variety of alcohols with O_2 over Au/CuO_{co}

Table 7 summarizes the catalytic results obtained on Au/CuO_{co} co-precipitated at pH 10 for the oxidation of a variety of alcohols. Similar conversion and selectivity were obtained for benzyl alcohol and its methyl-substituted derivatives under the employed reaction conditions (entries 1, 6, and 7). This shows that the presence of a methyl group in benzyl alcohol had no obvious effect on its reactivity. However, this is different for the cycloalcohols. A remarkable increase in the activity with increasing methyl groups was observed for the cyclohexanol and its derivatives with ketone selectivity higher than 99% (entries 3, 8, and 9). This also held true for the cycloalcohols (entries 3, 4, and 5). When cyclooctanol and cyclododecanol were oxidized, both the conversion and the ketone selectivity were higher than 99%. In contrast, cyclohexanol as substrate only gave a conversion of 66%. The tensions of cycloalcohol rings increase with their sizes or carbon atoms. This causes that the ring structure to be more unstable but more reactive. As a consequence, the conversions of cycolalcohols decreased in the order cyclododecanol > cyclooctanol > cyclohexanol. It is worth noting that the Au/CuO_{co} was also highly active and selective for the oxidation of unsaturated alcohols. The conversion of cinnamyl alcohol and the selectivity of cinnamyl aldehyde reached 83.8% and 99.4%, respectively (entry 2). These results show that the Au/CuO_{co} is effective at least for benzylic, cyclic, and unsaturated alcohols.

4. Conclusions

Au/CuO_{co} is highly active and selective for the oxidation of benzylic, cyclic, and unsaturated alcohols to the corresponding aldehydes or ketones by molecular oxygen at atmospheric pressure. When bulky cyclooctanol and cyclododecanol are oxidized, both the conversion and the ketone selectivity are higher than 99%. The preparation method and the pH value and stirring rate during the co-precipitation process have significant effects on the catalytic performance as a result of influencing the structure of the support and/or the electronic state and particle size of gold. The sample prepared by the co-precipitation method showed higher activity and selectivity than the samples prepared by the HCHO-reduction and impregnation methods. The optimum pH value and stirring rate during the co-precipitation process are 10 and 100 rpm, respectively. The Au/CuO_{co} is a stable heterogeneous catalyst and can be recycled to use with regeneration. Addition of alkali metal salts to the reaction mixture is not positive for the increase in the activity but in the catalytic stability. After being activated by Au nanoparticles, the benzyl alcohol molecule interacts with surface lattice oxygen of CuO to form bridged O—C—O group as intermediate, which is followed by the β-H elimination to form benzaldehyde and water.

Acknowledgments

The authors are grateful for financial support by the National Basic Research Program (Nos. 2011CB201403 and 2009CB226101), the National Science Foundation of China (Nos. 21273264, 21203231, and 20876163), and the Natural Science Foundation of Shanxi Province (Nos. 2009011009-2 and 2011011006-3).

Appendix A. Supplementary material

Supplementary data associated with this article can be found, in the online version, at http://dx.doi.org/10.1016/j.jcat.2012.11.018.

References

[1] D.I. Enache, J.K. Edwards, P. Landon, B. Solsona-Espriu, A.F. Carley, A.A. Herzing, M. Watanabe, C.J. Kiely, D.W. Knight, G.J. Hutchings, Science 311 (2006) 362.
[2] B. Zhan, A. Thompson, Tetrahedron 60 (2004) 2917.
[3] J.U. Ahmad, P.J. Figiel, M.T. Räisänen, M. Leskela, T. Repo, Appl. Catal. A 371 (2009) 17.
[4] C.P. Vinod, K. Wilson, A.F. Lee, J. Chem. Technol. Biotechnol. 86 (2011) 161.
[5] Z. Hou, N. Theyssen, A. Brinkmann, K.V. Klementiev, W. Grünert, M. Bühl, W. Schmidt, B. Spliethoff, B. Tesche, C. Weidenthaler, W. Leitner, J. Catal. 258 (2008) 315.
[6] A.S.K. Hashmi, Chem. Rev. 107 (2007) 3180.
[7] C. Milone, R. Ingoglia, A. Pistone, G. Neri, S. Galvagno, Catal. Lett. 87 (2003) 201.
[8] A. Abad, P. Concepción, A. Corma, H. García, Angew. Chem. Int. Ed. 44 (2005) 4066.
[9] G.J. Hutchings, Chem. Commun. (2008) 1148.
[10] X. Yang, X. Wang, C. Liang, W. Su, C. Wang, Z. Feng, C. Li, J. Qiu, Catal. Commun. 9 (2008) 2278.
[11] M. Haruta, Catal. Today 36 (1997) 153.
[12] D.C. Lim, R. Dietsche, G. Gantefor, Y.D. Kim, Appl. Surf. Sci. 256 (2009) 1148.
[13] G.C. Bond, C. Louis, D.T. Thompson, Catalysis by Gold, Imperial College Press, London, 2006. p. 80.
[14] A. Stephen, K. Hashmi, G.J. Hutchings, Angew. Chem. Int. Ed. 45 (2006) 7896.

[15] D.C. Lim, I. Lopez-Salido, R. Dietsche, M. Bubek, Y.D. Kim, Angew. Chem. Int. Ed. 45 (2006) 2413.
[16] H. Tsunoyama, H. Sakurai, Y. Negishi, T. Tsukuda, J. Am. Chem. Soc. 127 (2005) 9374.
[17] The Sadtler Handbook of Infrared Spectra, Informatics Division. Bio-Rad Laboratories, Inc., 1978–2004, pp. 120, 133 and 148.
[18] G. Socrates, Infrared Characteristic Group Frequencies: Tables and Charts, second ed., Wiley, England, 1997. pp. 80–103.
[19] B. Stuart, Infrared Spectroscopy: Fundamentals and Applications, Infrared Spectroscopy: Fundamentals and Applications, Wiley, England, 2004. p. 74.
[20] L. Piccolo, H. Daly, A. Valcarcel, F.C. Meunier, Appl. Catal. B 86 (2009) 190.
[21] C.P.M. Roelands, J.H. ter Horst, H.J.M. Kramer, P.J. Jansens, Cryst. Growth Des. 6 (2006) 1380.
[22] J. Cornel, C. Lindenberg, M. Mazzotti, Cryst. Growth Des. 9 (2009) 243.
[23] S. Higashimoto, N. Kitao, N. Yoshida, T. Sakura, M. Azuma, H. Ohue, Y. Sakata, J. Catal. 266 (2009) 279.
[24] V.D. Makwana, Y.C. Son, A.R. Howell, S.L. Suib, J. Catal. 210 (2002) 46.
[25] Y.T. Chen, H.J. Zheng, Z. Guo, C.M. Zhou, C. Wang, A. Borgna, Y.H. Yang, J. Catal. 283 (2011) 34.
[26] X.P. Xu, C.M. Friend, Surf. Sci. 260 (1992) 14.
[27] N. Gleason, J. Guevremont, F. Zaera, J. Phys. Chem. B 107 (2003) 11133.
[28] J. Gong, D.W. Flaherty, T. Yan, C.B. Mullins, ChemPhysChem 9 (2008) 2461.